# Drainage of a horizontal Boussinesq aquifer with a power law hydraulic conductivity profile

David E. Rupp and John S. Selker

Department of Bioengineering, Oregon State University, Corvallis, Oregon, USA

[1]   Solutions to the Boussinesq equation describing drainage into a fully penetrating channel have been used for aquifer characterization. Two analytical solutions exist for early- and late-time drainage from a saturated, homogeneous, and horizontal aquifer following instantaneous drawdown. The solutions for discharge $Q$ can be expressed as $dQ/dt = -aQ^b$, where $a$ is constant and $b$ takes on the value 3 and 3/2 for early and late time, respectively. Though many factors can contribute to departures from the two predictions, we explore the effect of having permeability decrease with depth, as it is known that many natural soils exhibit this characteristic. We derive a new set of analytical solutions to the Boussinesq equation for $k \propto z^n$, where $k$ is the saturated hydraulic conductivity, $z$ is the height above an impermeable base, and $n$ is a constant. The solutions reveal that in early time, $b$ retains the value of 3 regardless of the value of $n$, while in late time, $b$ ranges from 3/2 to 2 as $n$ varies from 0 to $\infty$. Similar to discharge, water table height $h$ in late time can be expressed as $dh/dt = -ch^d$, where $d = 2$ for constant $k$ and $d \to \infty$ as $n \to \infty$. In theory, inclusion of a power law $k$ profile does not complicate aquifer parameter estimation because $n$ can be solved for when fitting $b$ to the late-time data, whereas previously $b$ was assumed to be 3/2. However, if either early- or late-time data are missing, there is an additional unknown. Under appropriate conditions, water table height measurements can be used to solve for an unknown parameter.

## 1.   Introduction

[2]   There are few tools available for deriving aquifer characteristics at the field or watershed scale. An important one which has received renewed attention, probably due to its apparent simplicity, is the method of recession analysis proposed by *Brutsaert and Nieber* [1977]. In the method, stream flow recession data, or discharge $Q$, is related to the time rate of change in discharge $dQ/dt$ in order to eliminate time as the reference. *Brutsaert and Nieber* [1977] noted that several models for aquifer discharge can be expressed as

$$\frac{dQ}{dt} = -aQ^b, \qquad (1a)$$

where $a$ and $b$ are constants. A similar relationship may exist for the height of the water table $h$ [e.g., *Rupp et al.*, 2004]:

$$\frac{dh}{dt} = -ch^d, \qquad (1b)$$

where $c$ and $d$ are also constants.

[3]   The model used most often for interpreting the parameters in (1a) and (1b) is the Boussinesq equation for

an unconfined, horizontal aquifer draining into a fully penetrating channel (Figure 1) [*Brutsaert and Nieber*, 1977; *Brutsaert and Lopez*, 1998; *Parlange et al.*, 2001; *Rupp et al.*, 2004]. The Boussinesq equation is derived from Darcy's law and the Dupuit-Forchheimer assumption, and by neglecting capillarity above the water table. Given these assumptions, the flux $q$ [$L^2\ T^{-1}$] per unit aquifer width at any horizontal position $x$ in an aquifer is

$$q = -kh(\partial h/\partial x), \qquad (2)$$

where $k$ is hydraulic conductivity and $h = h(x, t)$ is the water table height. Applying the continuity equation in the presence of a recharge rate $N$ leads to

$$\varphi \frac{\partial h}{\partial t} = \frac{\partial}{\partial x}\left(kh\frac{\partial h}{\partial x}\right) + N, \qquad (3)$$

where $\varphi$ is the drainable porosity or specific yield. Typically, $k$ is moved outside of the derivative, as it is assumed spatially constant in the down-slope direction, and the result is referred to as the Boussinesq equation.

[4]   *Polubarinova-Kochina* [1962, p. 507] presented an analytical solution for (3) given constant $k$ following instantaneous drawdown of an initially saturated aquifer where $h(0, t) = 0$. For this solution, $b = 3$ in (1a), and it is applicable in "early time" when the no-flux boundary at $x = B$ is not yet affecting drainage at $x = 0$. The solution was arrived at by using the Boltzmann transfor-
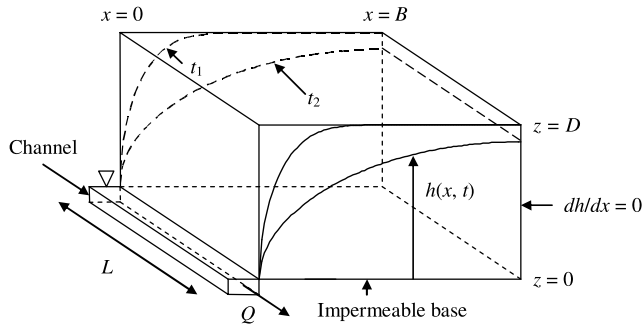
**Figure 1.** Diagram of the right-hand side of a symmetrical unconfined aquifer fully incised by a channel. Water table profiles at $t_1$ and $t_2$ correspond to early and late times during sudden drawdown of an initially saturated aquifer. The channel discharge $Q$ is the sum of the discharge from both sides of the aquifer, or $2qL$. The vertical axis is exaggerated with respect to the horizontal axis, but in reality $B \gg D$.

mation and further substitutions to express the Boussinesq equation in the form of the Blasius equation, for which there are known analytical solutions [see also *Heaslet and Alksne*, 1961; *Hogarth and Parlange*, 1999]. *Lockington* [1997] derived a similar early-time solution using a weighted residual method for the more general case where $h(0, t) \geq 0$ and is constant. For this latter solution, recast as (1a), $b = 3$ also.

[5] For "late time," when the no-flux boundary affects flow, an analytical solution can also be derived for the boundary condition $h(0, t) = 0$ by noting that the solution $h(x, t)$ is separable into the product of a function of $x$ and a function of $t$ [*Boussinesq*, 1904; *Polubarinova-Kochina*, 1962, pp. 516–517]. In this case, $b = 3/2$ in (1a). In the corresponding expression for water table decline (1b), $d = 2$.

[6] *Parlange et al.* [2001] provided an approximate analytical solution for discharge that unites the early- and late-time regimes.

[7] In natural basins and aquifers, there are many factors that can lead to departures from the predictions of outflow given by analytical solutions derived for the instantaneous drawdown of the idealized "lumped" aquifer depicted in Figure 1 [e.g., *Hall*, 1968; *Singh*, 1968]. Recent investigations have begun to quantify the effects of some of these factors by relaxing some of the previously mentioned assumptions. *Szilagyi et al.* [1998] examined the robustness of the two analytical solutions discussed above by including horizontal heterogeneity in saturated hydraulic conductivity, complexity in watershed shape, and mild slope in a numerical model. Others have compared solutions of the one-dimensional Boussinesq equation to the more general two-dimensional Laplace equation for a horizontal aquifer. In particular, the assumptions of initial saturation and instantaneous drawdown [*van de Giesen et al.*, 2005], full and partial penetration [*van de Giesen et al.*, 1994; *Szilagyi*, 2003; *van de Giesen et al.*, 2005], and no unsaturated flow [*Szilagyi*, 2003, 2004] were addressed.

[8] One aspect that has not been well studied within the context of the Boussinesq equation is the effect of saturated hydraulic conductivity that varies with depth. Vertically decreasing $k$ has been observed in many soil types [e.g.,

*Beven*, 1984], particularly in forests [e.g., *Harr*, 1977; *Bonell et al.*, 1981]. *Beven* [1982a] observed that the power law function $k = k^*z^n$ fits well to existing data from five previous studies. Where $z$ is the height above a relatively impermeable base and where $k^*$ and $n$ are fitting parameters, $n$ ranged from 1.2 to 7.9, with correlation coefficients $r$ between 0.85 and 0.97. In response, *Beven* [1982b] introduced a vertical $k$ profile that is a power law of $h$ into the Boussinesq equation for a sloping aquifer [*Boussinesq*, 1877], but eliminated the second-order diffusive term to arrive at a linear kinematic wave equation.

[9] We introduce a similar power law conductivity profile into (3) and derive early- and late-time analytical transient solutions for an initially saturated aquifer following instantaneous drawdown. We also present an analytical steady state solution under constant recharge. For verification, the analytical solutions are compared with numerical solutions of the Boussinesq equation. Last, we discuss how $k$ decreasing with depth may affect the derivation of aquifer characteristics using the recession slope analysis method of *Brutsaert and Nieber* [1977], or, in other words, how the power law $k$ profile affects the parameters in (1a) and (1b).

## 2. Analytical Solutions

[10] Let the saturated hydraulic conductivity $k$ at an elevation $z$ above the impermeable base be described by

$$k(z) = (k_D - k_0)\left(\frac{z}{D}\right)^n + k_0, \qquad (4)$$

where $D$ is the thickness of the aquifer, $k(D) = k_D$ and $k(0) = k_0$ are the constant values of $k$ at the upper and lower contacts, respectively, and $n \geq 0$. The average horizontal hydraulic conductivity corresponding to the entire saturated thickness of the aquifer $h$, or $k(h)$, is the vertical average of $k(z)$:

$$k(h) = \frac{1}{h}\int_0^h \left(\frac{k_D - k_0}{D^n}z^n + k_0\right)dz \qquad (5)$$

or

$$k(h) = k^*h^n + k_0 \qquad (6)$$

where

$$k^* = \frac{k_D - k_0}{(n+1)D^n}. \qquad (7)$$

### 2.1. Steady State Case

[11] We derive a steady state solution to (3) given (6) because it serves both as a test here of the numerical model and as a plausible condition when considering extended wet periods. The steady state solution of (3) requires that (2) be equal to a constant in time. Given a constant recharge rate $N$ applied uniformly across the water table, the conservation of mass requires that the steady state flux at $x$ is equal to the recharge contributed up-gradient of $x$, or

$$q = -N(B - x), \qquad (8)$$

where $B$ is the distance from the channel to the no-flow boundary (Figure 1). Substituting (6) and (8) into (2) gives

$$N(B - x) = (k^*h^n + k_0)h(\partial h/\partial x). \qquad (9)$$

Integrating the left side of (9) from $x = 0$ to $x = x$ and the right side from $h(0) = h_0$ to $h(x) = h$ yields an exact implicit solution in $x$:

$$N(2Bx - x^2) = \frac{2k^*}{n+2}h^{n+2} + k_0h^2 - \left(\frac{2k^*}{n+2}h_0^{n+2} + k_0h_0^2\right), \qquad (10)$$

where $h_0$ is the constant water level in the channel.

[12] In the following sections, two transient solutions to the Boussinesq equation will be derived for the special case where $h_0 = 0$ and $k_0 = 0$. Given these two boundary conditions, the steady state solution can be expressed for $h$ explicitly:

$$h = \left[\frac{(n+2)}{2k^*}N(2Bx - x^2)\right]^{1/(n+2)}. \qquad (11)$$

### 2.2. Early-Time Transient Case

[13] To arrive at analytical solutions for instantaneous drawdown and without recharge, we let $k_0 = 0$, so $k^* = k_D/[(1+n)D^n]$ and (2) and (3) become, respectively

$$q = -k^*h^{n+1}(\partial h/\partial x) \qquad (12)$$

$$\frac{\partial h}{\partial t} = \frac{k^*}{\varphi}\frac{\partial}{\partial x}\left(h^{n+1}\frac{\partial h}{\partial x}\right). \qquad (13)$$

[14] A weighted residual method [Lockington, 1997] is used to solve (13) for early time where the drawdown of the water table is not yet subject to the influence of the no-flux boundary at $x = B$ (see Figure 1, curve $t_1$). The aquifer can then be treated as being "semi-infinite" and the initial and boundary conditions are

$$h = 0 \qquad x = 0 \qquad t > 0 \qquad (14)$$

$$h = D \qquad x \geq 0 \qquad t = 0 \qquad (15)$$

$$h = D \qquad x \to \infty \qquad t > 0. \qquad (16)$$

The substitutions $\phi = x/\sqrt{\tau}$, $H = h/D$, and $\tau = k^*t/\varphi$ reduce (13) to the two-variable problem

$$-\frac{\phi}{2}\frac{dH}{d\phi} = D^{n+1}\frac{d}{d\phi}\left(H^{n+1}\frac{dH}{d\phi}\right) \qquad (17)$$

with boundary conditions

$$H = 0 \qquad \phi = 0 \qquad (18)$$

$$H = 1 \qquad \phi \to \infty. \qquad (19)$$

Integrating (17) with respect to $\phi$ yields

$$2D^{n+1}H^{n+1} = \int_H^1 \phi d\overline{H}\frac{d\phi}{dH} \qquad (20)$$

because $dH/d\phi$ vanishes at $H = 1$. $\overline{H}$ is a dummy variable of integration.

[15] The following approximate function $\phi^*$ used by Lockington [1997] for a homogeneous aquifer is proposed for $\phi$:

$$\phi \approx \phi^* = \lambda[(1 - H^{-\mu}) - 1], \qquad (21)$$

where $\lambda$ and $\mu$ are constants with the same sign. As $\phi^*$ is not an exact solution to (20), a residual function $\varepsilon(H)$ is defined as

$$\varepsilon = 2D^{n+1}H^{n+1} - \int_H^1 \phi^*(\overline{H})d\overline{H}\frac{d\phi}{dH}. \qquad (22)$$

The residual is weighted with 1 and $(1 - H)^m$ [Lockington, 1997] and integrated over the range of $H$ to solve for $\lambda$ and $\mu$:

$$\int_0^1 \varepsilon dH = 0 \qquad (23)$$

$$\int_0^1 (1 - H)^m \varepsilon dH = 0. \qquad (24)$$

From (23)

$$\lambda^2 = \frac{(1-\mu)(1-2\mu)}{\mu^2}\frac{D^{n+1}}{n+2} \qquad (25)$$

and from (24)

$$2D^{n+1}\mathrm{B}(n+2, m+1) = \frac{\lambda^2\mu^2(2 + m - 2\mu)}{(1 + m - \mu)(1 + m - 2\mu)}, \qquad (26)$$

where $\mathrm{B}(n + 2, m + 1)$ denotes the beta function evaluated for $n + 2$ and $m + 1$. Substituting (25) into (26) gives

$$\mathrm{A} = \frac{(1 - 2\mu)(2 + m - 2\mu)}{(1 + m - \mu)(1 + m - 2\mu)}, \qquad (27)$$

where

$$\mathrm{A} = 2(n + 2)\mathrm{B}(n + 2, m + 1). \qquad (28)$$

It can be shown by rearrangement that (27) is a quadratic equation. The useful root $\mu$ is that with real values of $H$ (and thus $h$)

$$\mu = \frac{-\beta - \sqrt{\beta^2 - 4\alpha\gamma}}{2\alpha} \qquad (29)$$

with

$$\alpha = 4 - 2A \tag{30}$$

$$\beta = 3A(m + 1) - 2m - 6 \tag{31}$$

$$\gamma = 2 + m - A(m + 1)^2. \tag{32}$$

The value $m = 1.251$ has been suggested for constant $k$ [*Lockington*, 1997]. However, if $m = 1$, the effect of which is discussed later, (29) becomes

$$\mu = \frac{4 - 3A - \sqrt{A^2 - 2A + 4}}{4 - 2A}, \qquad m = 1. \tag{33}$$

Finally, substituting (25) into (21) and solving for $H$, and making the substitutions $H = h/D$ and $\phi^* = x/\sqrt{k^*t/\varphi}$, yield the approximate water table profile

$$h(x,t) = D\left[1 - \left(1 + \mu\frac{x}{\sqrt{t}}\sqrt{\frac{(n+2)(n+1)\varphi}{(1-\mu)(1-2\mu)k_D D}}\right)^{-1/\mu}\right]. \tag{34}$$

[16] The outflow from the aquifer is the flux at $x = 0$. Evaluating (12) at $\phi = 0$, or

$$q = -k^*\tau^{-1/2}D^{n+2}H^{n+1}(dH/d\phi)|_{\phi=0} \tag{35}$$

gives, from (20),

$$q = -\frac{k^*D}{2\tau^{1/2}}\int_0^1 \phi(H)dH. \tag{36}$$

Substituting (21) and (25) into (36) and solving the integral yields the early-time outflow

$$q(t) = \frac{1}{2}\left[\frac{(1-2\mu)}{(1-\mu)(n+2)(n+1)}k_D\varphi D^3\right]^{1/2}t^{-1/2}. \tag{37}$$

### 2.3. Late-Time Transient Case

[17] A separation of variables is used to solve (13) for the late-time case where the drawdown of the water table is subject to the effect of the no-flux boundary at $x = B$ [*Boussinesq*, 1904; *Polubarinova-Kochina*, 1962] (see Figure 1, curve $t_2$). The boundary conditions are

$$h = 0 \qquad x = 0 \qquad t > 0 \tag{38}$$

$$dh/dx = 0 \qquad x = B \qquad t \geq 0 \tag{39}$$

$$h = D \qquad x = B \qquad t = 0. \tag{40}$$

We seek a solution for the free water surface $h$ which is the product of two variables, one dependent solely on time and the other solely on the position:

$$h = X(x)T(t). \tag{41}$$

Substituting (41) into (13) and separating the variables yields

$$\frac{1}{T^{n+2}}\frac{dT}{dt} = \frac{k^*}{\varphi X}\frac{d^2}{dx^2}\left(\frac{X^{n+2}}{n+2}\right) = -C, \tag{42}$$

where $C$ is a constant. The boundary conditions are

$$X = 0 \qquad x = 0 \qquad t > 0 \tag{43}$$

$$X = D \qquad x = B \qquad t = 0 \tag{44}$$

$$T = 1 \qquad t = 0. \tag{45}$$

Integrating the left and right sides of (42) give

$$T = [1 + (n+1)Ct]^{-1/(n+1)} \tag{46}$$

$$dx = \sqrt{\frac{k^*(n+3)}{2C\varphi}}\frac{X^{n+1}dX}{\sqrt{D^{n+3} - X^{n+3}}}, \tag{47}$$

respectively. Integrating (47) again yields

$$x = \frac{B}{B_n}\int_0^v v^{-1/(n+3)}(1-v)^{-1/2}dv, \qquad v = (X/D)^{n+3} \tag{48}$$

where $B_n$ is a beta function

$$B_n = B\left(\frac{n+2}{n+3}, \frac{1}{2}\right). \tag{49}$$

The integral in (48) is an incomplete beta function. A series expansion, for example, can be used to approximate the inverse of the incomplete beta function [see, e.g., *Abramowitz and Stegun*, 1972, equation 26.5.4].

[18] The constant $C$ subject to the boundary conditions is

$$C = \frac{k^*D^{n+1}}{2(n+3)\varphi B^2}B_n^2, \tag{50}$$

which is used to arrive at (48) above. From (41), (46), and (48), the water table height is

$$h(x,t) = \frac{D\Omega}{\left[1 + \frac{B_n^2}{2(n+3)}\frac{k_D D}{\varphi B^2}t\right]^{1/(n+1)}}, \tag{51}$$

where $\Omega(x/B) = X/D$. Examples of water table profiles for various values of $n$ at $t = 0$ are shown in Figure 2.

[19] The outflow from the aquifer can be found from (12) evaluated at $x = 0$:

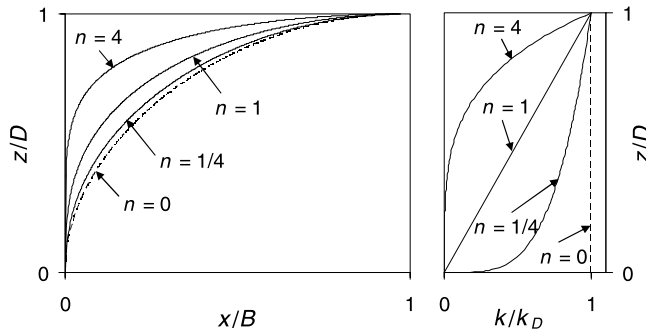$$q = -k^*T^{n+2}X^{n+1}(dX/dx)|_{x=0} \tag{52}$$

**Figure 2.** (left) Dimensionless late-time transient water table profiles $h(x, 0)/D$ in an unconfined aquifer with a fully penetrating channel at $x = 0$. The water table heights shown are calculated from the late-time solution (51) for $t = 0$ and four vertical profiles of saturated hydraulic conductivity $k$ corresponding to $n = 0, 1/4, 1$, and 4. (right) Dimensionless hydraulic conductivity $k(z)/k_D$ versus dimensionless height $z/D$ above the impermeable base.

Combining (47) with (52) and letting $X = 0$ gives

$$q(t) = \frac{B_n k_D D^2}{(n+3)(n+1)B\left[1 + \frac{B_n^2}{2(n+3)}\frac{k_D D}{\varphi B^2}t\right]^{\frac{n+2}{n+1}}}. \qquad (53)$$

## 3. Discussion

[20] For permeability that varies as a power function with depth, both the early-time (equation (37)) and late-time (equation (53)) solutions for discharge can be expressed in the form given by (1a). Taking the derivative of (37) with respect to time and recasting the result as a function of discharge instead of time, the recession constants $a$ and $b$ for the early-time solution are

$$a_1 = \Phi_1 \frac{(n+1)}{k_D \varphi D^3 L^2} \qquad (54)$$

$$b_1 = 3 \qquad (55)$$

where

$$\Phi_1 = \frac{(1-\mu)(n+2)}{2(1-2\mu)}. \qquad (56)$$

Values of $\Phi_1$ for various values of $n$ are given in Table 1. Note also that the discharge $Q$ in the channel is assumed to be the cumulative outflow from all upstream aquifers such that $Q = 2qL$ (see Figure 1).

[21] Defining the width of the aquifer $B$ as the characteristic distance from channel to divide, the aquifer area $A$ is given by $A = 2LB$. The recession parameters for the late-time solution (53) can then be expressed as

$$a_2 = \Phi_2 \frac{4k_D D L^2}{(n+1)\varphi A^2}\left[\frac{(n+1)A}{4k_D D^2 L^2}\right]^{\frac{n+1}{n+2}} \qquad (57)$$

$$b_2 = (2n+3)/(n+2), \qquad (58)$$

where

$$\Phi_2 = \frac{n+2}{2(n+3)}B_n^2\left[\frac{n+3}{B_n}\right]^{\frac{n+1}{n+2}}. \qquad (59)$$

See Table 1 for values of $b_2$ and $\Phi_2$ for various values of $n$.

[22] Unlike for discharge, the Boussinesq equation does not predict a power law relationship between $dh/dt$ and $h$ in early time. However, the late-time solution (51) can be expressed in the form of (1b) with constants

$$c = \frac{B_n^2}{2(n+3)(n+1)}\frac{k_D}{\varphi D^n B^2 \Omega^{n+1}} \qquad (60)$$

$$d = n + 2. \qquad (61)$$

[23] The analytical solutions derived above were compared to output from a numerical model of (23) using a fourth-order Runge-Kutta finite difference method with 250 equally spaced nodes in the $x$-direction. Numerical outflow hydrographs were generated for various values of $n$, $k_D$, and $D$. The data were plotted as $\log(-dQ/dt)$ versus $\log(Q)$, as proposed by *Brutsaert and Nieber* [1977] (see also *Rupp and Selker* [2005] for discussion on the numerical approximation of $\log(-dQ/dt)$ versus $\log(Q)$ from discrete data). Plotted in log-log space, the analytical solutions appear as straight lines with slope $b$ and intercept $a$. Three numerically generated recession curves are given as examples in Figure 3.

[24] The early-time slope $b$ for discharge of the numerical simulations was not perceptibly different from 3 regardless of the value of $n$. It was observed, however, that the node spacing had to be decreased for large $n$, or else $b$ appeared as less than 3 for very early times and gradually approached a value of 3 (data not shown). Therefore the node spacing was reduced by a factor of 10 to obtain just the early-time data for the largest values of $n$. The number of nodes was maintained at 250, as the early-time solution is not a function of the position of the no-flux boundary at $x = B$.

[25] Following the sharp transition from the early- to late-time regime, the numerically generated data show a slope $b$ that is equal to that predicted by the late-time solution (58) (Figure 3). For late time, the initial node spacing was adequate for all $n$.

[26] In addition to the slope $b$, the analytically and numerically generated recession curves are nearly identi-

**Table 1.** Recession Coefficients for Various Vertical Hydraulic Conductivity Profiles, $k \propto z^n$

| | Early Time ($b = 3$) | Late Time | |
|---|---|---|---|
| $n$ | $\Phi_1$ (56) ($m = 1$) | $\Phi_2$ (59) | $b_2$ (58) |
| 0 | 1.108 | 2.402 | 1.500 |
| $1/4$ | 1.337 | 2.538 | 1.556 |
| $1/2$ | 1.588 | 2.690 | 1.600 |
| 1 | 2.151 | 3.030 | 1.667 |
| 2 | 3.528 | 3.787 | 1.750 |
| 4 | 7.279 | 5.445 | 1.833 |
| 64 | 739.8 | 63.17 | 1.971 |
| $\infty$ | $\infty$ | $\infty$ | 2.000 |

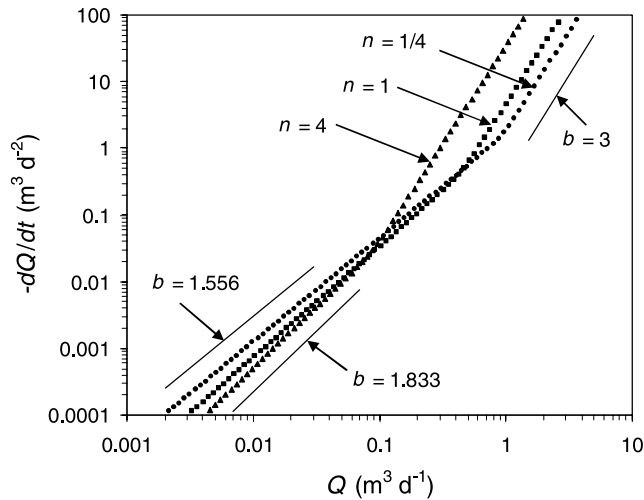**Figure 3.** Recession curves from three numerical simulations using saturated hydraulic conductivities that decrease with depth from $k_D = 100$ m d$^{-1}$ to $k_0 = 0$ m d$^{-1}$ slowly ($n = 0.25$), linearly ($n = 1$), and rapidly ($n = 4$). In each case $D = 1$ m, $B = 100$ m, $\varphi = 0.01$, and $L = 1$ m. The analytically derived values of $b$ are shown for $n = 0.25$ and $n = 4$.

cally positioned in log-log space for late time (i.e., the values of the parameter $a_2$ are equal). There is a discrepancy, however, in early time. Using a value of $m = 1.251$ for (24) [*Lockington*, 1997] to calculate $a_1$ from (54), the numerical and analytical solutions diverge for increasing $n$ (Figure 4). For small $n$ (e.g., $n \leq 1$), this may not have practical consequences. However, for the example show in Figure 4a, the difference in $a_1$ between the solutions is about 15% for $n = 4$ and 40% for $n = 32$. The discrepancy does not appear to be due to numerical error, as changing the node spacing or the time step did not result in a convergence of predictions. On the other hand, if we let $m = 1$, the analytically and numerically derived values of $a_1$ show a much better match, with the difference being about 1% for all $n$ (Figure 4).

[27] Accurate estimates of $\Phi_1$ in (54) are known for $n = 0$, so comparisons can be made to the value predicted by (56) for this specific case. The most accurate value of $\Phi_1$, to the fourth decimal place, is 1.1337 [see *Parlange et al.*, 2001]. In comparison, for $n = 0$, (57) gives $\Phi_1 = 1.1361$ for $m = 1.251$ and $\Phi_1 = 1.1076$ for $m = 1$. Thus the value of $m$ proposed by *Lockington* [1997] is superior to $m = 1$ for very small $n$, but performs poorly over all $n$. One might apply a correction factor to (56) for $m = 1$ to improve the prediction at $n = 0$, though this may not be justified for the purposes of recession slope analysis in log-log space.

[28] It is remarkable that the recession parameter $b$ retains the value of 3 in early time regardless of the shape of the $k$ profile. The practical implication of this result for aquifer characterization is that the shape of the early-time outflow hydrograph alone gives no indication of vertical variability in $k$, thus adding at least one unknown variable to the parameterization problem. However, if late-time data are also available, the late-time value of $b$ supplies information on the vertical variability in $k$ (i.e., $n$), thus the problem of parameterization is in theory no more complicated than for the case of constant $k$ with two equations and the same number of unknowns. (If, however, the vertical $k$ profile

were defined with an extra parameter, such as in (6), there would be another variable for which to solve).

[29] Though the early- and late-time curves can be used together to solve for an unknown parameter by combining (54) and (57), it is likely that the predicted early-time response will not be evident in discharge data. This is because the assumption of sudden drawdown from an initially flat water table may be inappropriate for the data being analyzed [*van de Giesen et al.*, 2005] or that observations during the early period of recession may still be reflecting processes other than merely aquifer outflow [*Brutsaert and Nieber*, 1977; *Brutsaert and Lopez*, 1998]. Furthermore, in the common case when only daily data are available, the temporal resolution may be too coarse to discern a relatively short lived early-time regime.

[30] From only the late-time data, estimating the characteristics of an aquifer with a power law $k$ profile requires solving for six variables, which is two more than for the case of a homogeneous aquifer (note that $D$ falls out of (57) for $b = 3/2$ or $n = 0$). When available, representative
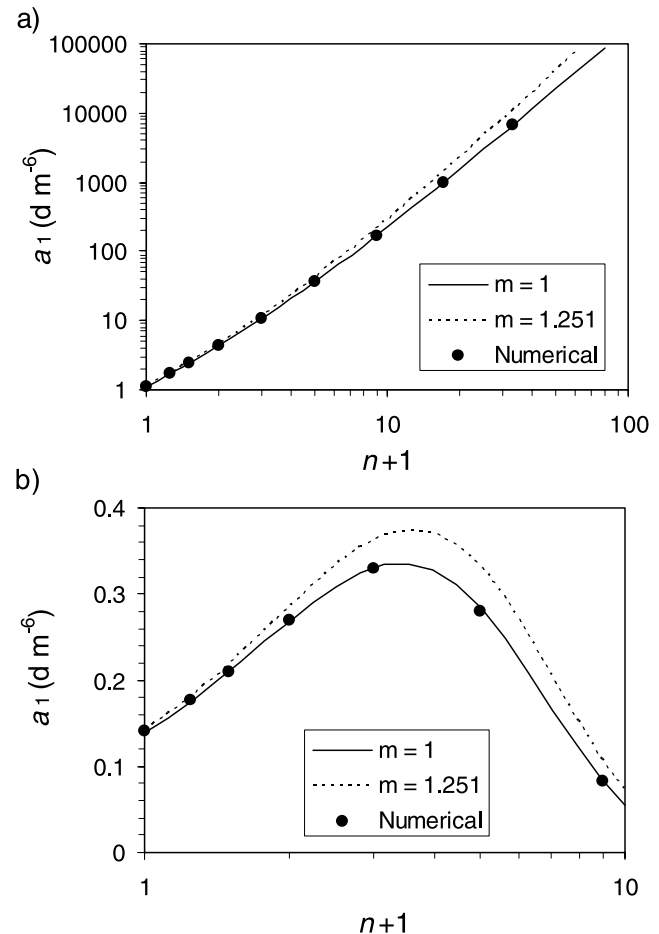


**Figure 4.** Early-time recession parameter $a$ from (1a) as determined analytically (lines) from (55) with two values of $m$ and numerically (circles) for various vertical profiles of saturated hydraulic conductivity. In Figure 4a, $k_D/D$ was held constant as $n$ was varied, with $k_D = 100$ m d$^{-1}$, $D = 1$ m, $B = 100$ m, $\varphi = 0.01$, and $L = 1$ m. In Figure 4b, $k_D/D^n$ was held constant at 100 m$^{1-n}$ d$^{-1}$ as $n$ was varied, with $D = 2$ m, and $B$, $\varphi$, and $L$ as above.

transient water table data can constrain the parameter space through the combination of (57) and (60) [e.g., *Rupp et al.*, 2004]. Water table observations may be especially useful for determining if there is important vertical variability in $k$, given that the parameter $d$ in (61) corresponding to the transient water table height is much more sensitive to $n$ than is the discharge parameter $b_2$ in (58).

[31] It has been shown previously that three values of $b$ arise out of three analytical solutions to the Boussinesq equation for a homogeneous aquifer [*Brutsaert and Nieber*, 1977]. As noted above, two of these values are $b = 3$ for early time and $b = 3/2$ for late time. The parameter $b$ also takes on a third value of 1 for a solution resulting from a linearization in $h$ in (3). Given that actual streamflow recession hydrographs show a range of values for $b$ and are thus not limited to 1, 3/2, and 3, there is interest in finding theoretical solutions for basin discharge that give other values of $b$.

[32] We have shown above how $b$ may take on any value between 3/2 and 2 and may also take on a value of 3 when the saturated hydraulic conductivity decreases with depth as a power law. It is interesting to compare our results to those of *Michel* [1999], who used dimensional considerations to arrive at an expression for aquifer discharge for any arbitrary value of $b$.

[33] *Michel* [1999] demonstrated that the three analytical solutions for a homogeneous aquifer can all be expressed in the form of (1a) through a single equation:

$$a = -\Psi(b)\frac{4kDL^2}{\varphi A^2}\left[\frac{A}{4kD^2L^2}\right]^{b-1} \qquad (62)$$

$$b = 1, 3/2, \text{ or } 3. \qquad (63)$$

Though there are only three known theoretical values of the coefficient $\Psi$, one each for $b = 1$, 3/2, and 3, *Michel* [1999] and *Brutsaert and Lopez* [1999] suggest functional forms for $\Psi(b)$, so that one might use (62) for any value of $b$. *Brutsaert and Lopez* [1999], for example, give

$$\Psi(b) = -10.513 + 15.030b^{1/2} - 3.662b. \qquad (64)$$

However, *Brutsaert and Lopez* [1999] recommend using caution when interpreting the recession parameter $a$ through (62) and (64) for values of $b$ different from 1, 3/2, and 3.

[34] It is of interest to compare (62) and (64) to the new solutions for a nonconstant $k$ profile. Noting that $b - 1 = (n + 1)/(n + 2)$, it is clear that (62) and the late-time solution (57) for a power law $k$ profile are nearly identical in form. The late-time coefficient $\Phi_2$ could also be expressed as function of $b$, as is $\Psi$. However, $\Phi_2$ is functionally very distinct from $\Psi$ (see also Table 1). In fact, $\Phi_2 \to \infty$ as $b \to 2$ (or as $n \to \infty$), whereas as $\Psi$ in (64) has no such singularity. Moreover, though (62) for $b = 3$ is also similar in form to the early-time solution (54) for a power law $k$ profile, the early-time coefficient $\Phi_1$ is not a function of $b$ at all. Given that our results do not support the functional forms for the coefficient $\Psi(b)$ proposed by *Michel* [1999] and *Brutsaert and Lopez* [1999], it appears that the use of (62) with an "empirically

derived" equation such as (64) without understanding why $b$ takes on a certain value is not justified.

## 4. Conclusion

[35] Recession hydrographs can differ in shape from those predicted by existing analytical solutions to the Boussinesq equation. In some cases, the initial and boundary conditions used to arrive at the analytical solutions may not be suited to the situation under analysis [e.g., *van de Giesen et al.*, 2005]. In other cases, the assumptions of the Boussinesq equation may be inappropriate. In this study, we investigated the effect of deviating from the assumption of an aquifer with constant saturated hydraulic conductivity $k$.

[36] It was found that for a power law vertical conductivity profile, the recession discharge in early time can be expressed as $dQ/dt \propto Q^3$, which is the same as the case of a homogeneous aquifer. In late time, however, the relation is $dQ/dt \propto Q^b$, where $b$ is a function of the exponent $n$ that defines the $k$ profile ($k \propto z^n$). The value of $b$ is 3/2 for a homogeneous aquifer ($n = 0$) and increases to 2 as $n$ approaches $\infty$. Observed values of $b$ exceeding 3/2 thus might be an indication of important decreases in $k$ with depth within an aquifer.

[37] The analytical solutions derived here for discharge allow for the derivation of aquifer characteristics much in the same way as that proposed by *Brutsaert and Nieber* [1977], with only slightly more complexity. The addition of transient water table data, analyzed in the same manner as that of discharge, can address some of the added complexity. It is acknowledged, however, that the analytical solutions assume that $k = 0$ at the base of the aquifer and thus may only be suitable for $k(D) \gg k(0)$.

## Notation

$a, b$    general discharge recession constants.
$a_1, b_1$    early-time discharge recession constants.
$a_2, b_2$    late-time discharge recession constants.
$A$    horizontal aquifer area, equal to $2LB$.
$B$    length of impermeable base of aquifer.
$c, d$    late-time water table recession constants.
$C$    constant of integration.
$D$    aquifer thickness.
$h$    water table height.
$h_0$    water table height at channel ($x = 0$).
$H$    dimensionless water table height, equal to $h/D$.
$\overline{H}$    dummy variable of integration.
$k$    saturated hydraulic conductivity.
$k_0$    saturated hydraulic conductivity at bottom of aquifer.
$k_D$    saturated hydraulic conductivity at top of aquifer.
$k^*$    coefficient, equal to $(k_D - k_0)/[(n + 1)D^n]$.
$L$    channel or stream length.
$m$    exponent in weight of residual; see (24).
$n$    exponent in expression for vertical profile of hydraulic conductivity.
$N$    rate of aquifer recharge.
$q$    aquifer discharge per unit width of aquifer.
$Q$    aquifer discharge.
$t$    time.
$T$    arbitrary function of $t$ only.
$v$    transform, equal to $(X/D)^{n+3}$.

$x$    horizontal coordinate.

$X$    arbitrary function of $x$ only.

$z$    elevation above aquifer base.

$\alpha,\ \beta,\ \gamma$    coefficients in quadratic equation.

$A$    function of $n$, equal to $2(n+1)B(n+2, m+1)$.

$B(,)$    beta function.

$B_n$    beta function evaluated for $(n+1)/(n+2)$, $1/2$.

$\varepsilon$    residual function, defined in (22).

$\phi$    Boltzmann transform, equal to $x/\sqrt{\tau}$.

$\phi^*$    approximate function for $\phi$, defined in (21).

$\Phi_1$    early-time discharge recession coefficient, defined in (56).

$\Phi_2$    late-time discharge recession coefficient, defined in (59).

$\lambda,\ \mu$    coefficients in function $\phi^*$.

$\varphi$    drainable porosity, or specific yield.

$\tau$    transformed time, equal to $\tau = k^*t/\varphi$.

$\Omega$    inverse of the normalized incomplete beta function, equal to $X/D$.

$\Psi$    discharge recession coefficient for homogeneous aquifer; see (62).

# References

Abramowitz, M., and I. A. Stegun (Eds.) (1972), *Handbook of Mathematical Functions*, 1046 pp., Dover, Mineola, N. Y.

Beven, K. (1982a), On subsurface stormflow: An analysis of response times, *Hydrol. Sci. J.*, 27, 505–521.

Beven, K. (1982b), On subsurface stormflow: Predictions with simple kinematic theory for saturated and unsaturated flows, *Water Resour. Res.*, 18, 1627–1633.

Beven, K. (1984), Infiltration into a class of vertically non-uniform soils, *Hydrol. Sci. J.*, 29, 425–434.

Bonell, M., D. A. Gilmour, and D. F. Sinclair (1981), Soil hydraulic properties and their effect on surface and subsurface water transfer in a tropical rainforest catchment, *Hydrol. Sci. Bull.*, 26, 1–18.

Boussinesq, J. (1877), Essai sur la théorie des eaux courantes, *Mem. Acad. Sci. Inst. Fr.*, 23, 252–260.

Boussinesq, J. (1904), Recherches théoriques sur l'écoulement des nappes d'eau infiltrées dans le sol et sur débit de sources, *J. Math. Pures Appl., 5me Ser.*, 10, 5–78.

Brutsaert, W., and J. P. Lopez (1998), Basin-scale geohydrologic drought flow features of riparian aquifers in the southern Great Plains, *Water Resour. Res.*, 34, 233–240.

Brutsaert, W., and J. P. Lopez (1999), Reply to comment on "Basin-scale geohydrologic drought flow features of riparian aquifers in the southern Great Plains," *Water Resour. Res.*, 35, 911.

Brutsaert, W., and J. L. Nieber (1977), Regionalized drought flow hydrographs from a mature glaciated plateau, *Water Resour. Res.*, 13, 637–643.

Hall, F. R. (1968), Base-flow recessions: A review, *Water Resour. Res.*, 4, 973–983.

Harr, R. D. (1977), Water flux in soil and subsoil on a steep forested hillslope, *J. Hydrol.*, 33, 37–58.

Heaslet, M. A., and A. Alksne (1961), Diffusion from a fixed surface with a concentration-dependent coefficient, *J. Soc. Ind. Appl. Math.*, 9, 584–596.

Hogarth, W. L., and J. Y. Parlange (1999), Solving the Boussinesq equation using solutions of the Blasius equation, *Water Resour. Res.*, 35, 885–887.

Lockington, D. A. (1997), Response of unconfined aquifer to sudden change in boundary head, *J. Irrig. Drain. Eng.*, 123, 24–27.

Michel, C. (1999), Comment on "Basin-scale geohydrologic drought flow features of riparian aquifers in the southern Great Plains" by W. Brutsaert and J. P. Lopez, *Water Resour. Res.*, 35, 909–910.

Parlange, J. Y., M. B. Parlange, T. S. Steenhuis, W. L. Hogarth, D. A. Barry, L. Li, F. Stagnitti, A. Heilig, and J. Szilagyi (2001), Sudden drawdown and drainage of a horizontal aquifer, *Water Resour. Res.*, 37, 2097–2101.

Polubarinova-Kochina, P. Y. (1962), *Theory of Ground Water Movement*, 613 pp., Princeton Univ. Press, Princeton, N. J.

Rupp, D. E., and J. S. Selker (2005), Information, artifacts, and noise in dQ/dt-Q recession analysis, *Adv. Water Resour.*, in press.

Rupp, D. E., J. M. Owens, K. L. Warren, and J. S. Selker (2004), Analytical methods for estimating saturated hydraulic conductivity in a tile-drained field, *J. Hydrol.*, 289, 111–127.

Singh, K. P. (1968), Some factors affecting baseflow, *Water Resour. Res.*, 4, 985–999.

Szilagyi, J. (2003), Sensitivity analysis of aquifer parameter estimations based on the Laplace equation with linearized boundary conditions, *Water Resour. Res.*, 39(6), 1156, doi:10.1029/2002WR001564.

Szilagyi, J. (2004), Vadose zone influences on aquifer parameter estimates of saturated-zone hydraulic theory, *J. Hydrol.*, 286, 78–86.

Szilagyi, J., M. B. Parlange, and J. D. Albertson (1998), Recession flow analysis for aquifer parameter determination, *Water Resour. Res.*, 34, 1851–1857.

van de Giesen, N., J. Y. Parlange, and T. S. Steenhuis (1994), Transient flow to open drains: Comparison of linearized solutions with and without the Dupuit assumption, *Water Resour. Res.*, 30, 3033–3039.

van de Giesen, N., T. S. Steenhuis, and J. Y. Parlange (2005), Short- and long-time behavior of aquifer drainage after slow and sudden recharge according to the linearized Laplace equation, *Adv. Water Resour.*, in press.

—————————————

D. E. Rupp and J. S. Selker, Department of Bioresource Engineering, Oregon State University, 116 Gilmore Hall, Corvallis, OR 97331, USA. (david.rupp@lifetime.oregonstate.edu)